The Effect of Solvent Evaporation in the Formation of Symmetric and Asymmetric Membranes with the Crystallization Polymer of EVAL

Abstract

The effect of evaporation process is investigated in the inversion of induced non-solvent phase in the poly system (ethylene alcohol-co-vinyl) (EVAL)/DMSO/ water. The duration of evaporation process is associated with membrane morphology resulting from the electron microscopy. Surprisingly, the evaporation time not only plays an important role in the creation of large pores, but also affects the membrane morphology from the sponge structure to the particle structure. The large pores are found in the membrane if the mold is immediately immersed in the water bath or the evaporation time is less than 15 minutes, while the large pores are reduced with the evaporation time of 30 minutes and the sponge structure is appeared. When the evaporation times are 45 and 60 minutes, a symmetrical membrane containing a packed bed of particles is observed with an equal diameter which is dominated by the solid-liquid separation process. This indicated that the polymer crystallization of EVAL from the evaporated solution prevents the formation of asymmetric membrane with cell pores dominated by liquid-liquid separation process. A crystallization process depends on the depth of solid-liquid separation region compared to the corresponding phase diagram. The results of the study showed that the membrane structure can be well controlled by understanding the mechanism of membrane formation.

1. Introduction

The importance of polymer membrane technologies is very famous in the separation industries [1]. The most production of commercial membrane is based on the inversion process stage of the induced non-solvent phase [2]. For a given polymer system, the membrane structure determines the separation characteristics. The basic principle of a membrane structures control from a crystallization polymer is the competition of liquid – liquid and solid-liquid separation process. Liquid-liquid separation results in the typical cell morphology. The solid-liquid separation is derived from the crystallization of the regular part of polymer. It has particle properties for the membrane morphology [3-9]. In the laboratory, we prepare poly membranes (ethylene alcohol-co-vinyl) (EVAL) with the particle morphology properties by the packed bed of particles with the approximately equal diameter of about a few microns [8-10]. Such particle membranes are useful in the separation of plasma protein [11] and microfiltration [12]. The competition between liquid-liquid and solid-liquid separation is understandable through the aspects of thermodynamics (phase behavior) and kinetics (mass transition) of immersion-deposition process [13, 9-15]. The phase diagram of ternary system, water-EVAL-DMSO is previously described at $25^0 C$ [8]. As shown in figure 1, there exists one single-phase area and two double-phase areas within the triangle (solid-liquid separation and liquid-liquid separation). Liquid-liquid separation boundary (e.g., double-knot) is within the solid-liquid separation. So, if a casting solution consists of a combination in the solvent / polymer axes of one-phase area which is shown in the point A, the casting solution enters to the liquid-liquid separation area after immersing to the bath deposition and before entering to the solid-liquid separation area. However, apart from thermodynamics, kinetics also plays an

important role in the formation of membranes. The liquid-liquid separation usually proceeds very quickly. While, the polymer crystallization always results in a certain degree of freezing and thus highly depends on the exchange rate of the solvent / non-solvent. Therefore, if mass transfer is very fast, solid-liquid separation may be ignored and the casting solution may be remain homogeneous until the entering of two-knot. As a result, liquid-liquid separation may occur for the first time to dominate the structure of the membrane. On the other hand, if the mass transfer is not rapid, the polymer has the opportunity to become supersaturated with respect to the crystallization and nuclear crystallization that occurs probably at the time of membrane formation.

In general, before entering the liquid-liquid separation, the available membrane solution in the solid-liquid separation area is important for the determination of the occurred stage. For example, when two systems have the same diffusion kinetics, the system has more time to crystallize the polymer with the large distance in the equilibrium crystallization line and two knots. Conversely, when the two systems have the same phase behavior, the system has more time to crystallize the polymer with kinetics distance of slower diffusion. Presentation of an evaporation process has the same effect on the rise time of the membrane solution in the solid-liquid separation area.

After removing the solvent, the sample A in the figure 1 can move to the position B located on the equilibrium crystallization and the border of two knots. Since, the supersaturated solution remains for a long time, there is an opportunity to crystallize the polymer. Thus, the aim of this paper is to examine whether crystal atom caused by the evaporation process may lead to change in membrane structure in the subsequent immersions in the non-solvent bath. The experiments are conducted in order to assess the membrane morphology of EVAL as a function of evaporation period.

Although, there are several models to describe the solvent evaporation of the membrane formation [16-19], the validity of these models is limited only to the amorphous polymer membrane. This theory is not satisfactory to explain the membrane formation of the crystallization polymers. Moreover, in a previous article, we assess the effect of the short time (5 minutes) and long time (1 day) of the evaporation process in the membrane structure from the supersaturated polymer solution [20]. However, it is not clearly analyzed the effect of crystallization on the structure of different membranes according to the duration changes of evaporation process. This study provides a basic understanding of the effects of evaporation process in the formation of asymmetric and symmetric membrane with crystallization polymer of EVAL.

Figure 1: Phase diagram of water-DMSO-EVAL system at the $25^0 C$ [8]. (━ Crystallization equilibrium line; ___ the border of two knots).
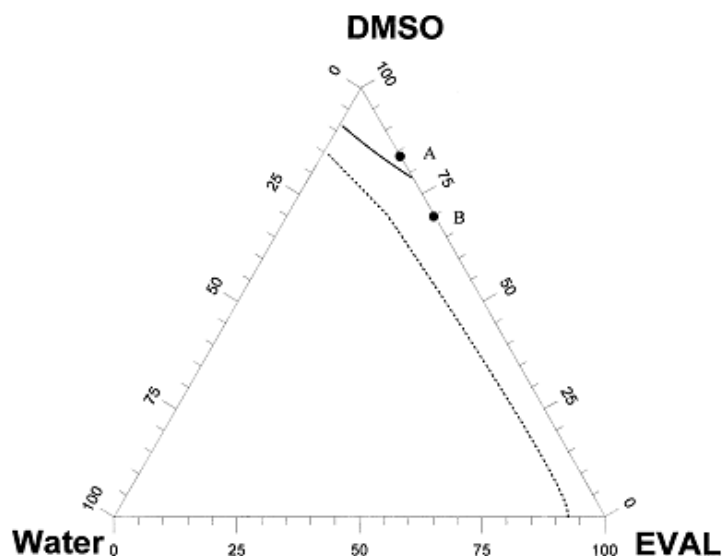
2. Experimental Section

1.2 Preparation of Membrane

The membrane is prepared using EVAL (105A, Kuraray, Japan) with a mean value of 44% ethylene mole. DMSO is used from the extra pure reagent-grade (Nacalai Tesque, Kyoto, Japan) as a solvent for EVAL. The non-solvent is deionized for the EVAL of the twice distilled water.

The EVAL membrane is prepared from the 15wt. % Of EVAL solution. This solution is released evenly on a glass plate (about 100) by an automatic mixer (KCC303, RK printing machine, UK). Since, the evaporation rate of DMSO is very low, the casting solution is evaporated in the vacuum furnace at a 6cm pressure of the mercury. The plate weight is recorded with the casting solution before and after a period of evaporation time in order to assess the changes in the composition of the casting solution.

Then, we fully immerse the evaporated solution in a water bath until the full formation of immersed membrane. All of the stages are performed at $25^0 C$. These prepared membranes on the dry ice samples are studied in order to observe the transition from finger to sponge and sponge to particle morphology using scanning electron microscopy (SEM).

2. Testing of Light Transmission

The light transmission tests are performed by measuring the advent time of optical homogenization of the casting solution in a water bath. The principle is that the light transmission is reduced due to the light homogenization that can be caused by liquid-liquid or solid-liquid separation. So, when the light transmission begins to reduce, it can be used to show the onset time of phase separation

from the casting solution in the water bath. To test the light transmission, a lamp is placed over the bath deposition as a light source and a light detector is used below the water bath to measure the light transmission. For more details about experimental setup and methods, see the work of Reuvers et al [13].

In addition, the light transmission experiment is conducted before the evaporation process in order to assess the possible effect of evaporation process in the emergence of light homogenization in the evaporated solution and no difference was evident.

3. Results

1.3 Evaporation of the Solvent

Figure 2 indicates the weight fraction of EVAL due to the loss of DMSO as a function of evaporation time. These data are determined by measuring the change in the weight of evaporated solution by gravimetric method. It should be noted that the concentration gradient must be present in the casting solution during the evaporation [21].

For simplicity, it is assumed that there is a flat concentration profile in the casting solution during the low fluctuations of DMSO removal of the casting solution level that can be compensated by the DMSO diffusion from the internal casting solution to the surface. This assumption will be further evaluated and justified in the section 4.

Figure 2: Weight fraction of EVAL from a solution of 15% w.t EVAL after different times of solvent evaporation.

4
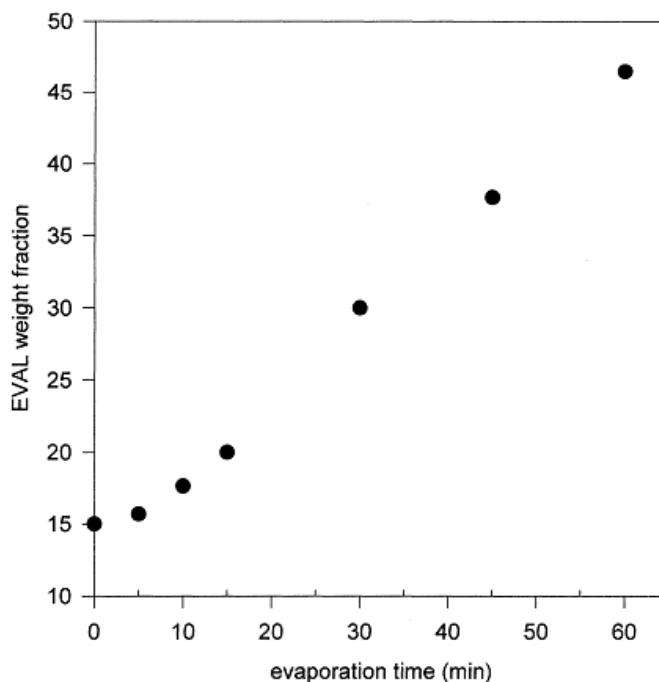
2.3 Light Transmission

Figure 3 indicates the light transmission characteristics for the sediment of a 15 wt% solution of EVAL in the water bath after different times of solution evaporation. It seems that all of the intensity of the light transmission from the membrane solution are reduced about 50% after immersion for 10 seconds. Therefore, immediate separation exists in all of the membrane formation cases. Before the immersion of evaporated solution in the water bath, the weight fraction of EVAL is in the 0.15-0.47 range (figure 2). This shows that since the dynamic of membrane formation is determined by the solvent and non-solvent emission rate, both of the diffusion coefficients of DMSO and water in the water/EVAL/DMSO system can be effectively proven in the range of 0.15 < EVAL concentration<0.47.

Figure 3: Light transmission characteristics for the sediment of a 15 wt% solution of EVAL in the water bath after different times of solution evaporation
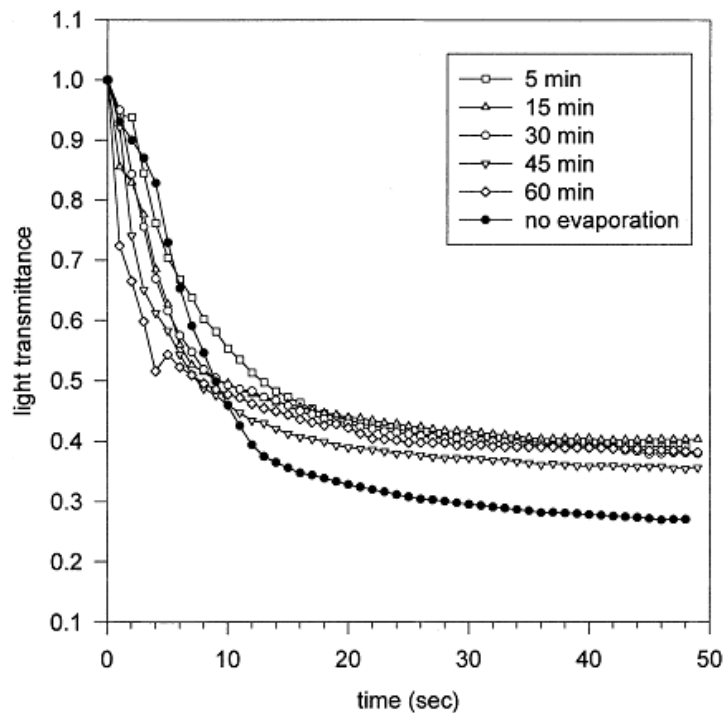

3.3 Morphological Studies

Figures 4-7 show the SEM images associated with membranes under different times of evaporation. There are six sets of images that cover the entire spectrum of evaporation-time. Figure 4 shows the membrane morphology for the direct immersion of casting solution in a water bath without evaporation stage. Figure 4(a) shows that the high-level of this membrane has a tight morphology.

Figure 4 (b) shows the backup layer containing finger-like large pores that almost extends to the bottom surface. In addition, the cross-sectional area near the top layer at higher magnification shows a thin and dense skin layer and encapsulated cell pores in a polymeric matrix which are similar to the amorphous membrane. The cellular structures are evidence of liquid-liquid

5

separation mechanism. Thus, the process of separation phase governing the membrane formation is liquid-liquid separation. However, figure 1 shows the double border below the equilibrium crystallization of the diagram phase of water-EVAL-DMSO at $25^0 C$. There is an expectation of induced crystallization morphology in the membrane because the crossing compound path from the equilibrium crystallization is ahead of two-knots. However, the morphology characteristic of polymer crystallization (e.g. particle, previously discussed in the [3-9]) is not observed within the membrane. This shows that the induction time is not long enough for separation of solid-liquid to the kernel. It is in consistent with immediate turbidity observed in the measurement of light transmission (Figure 3). Thus, membrane structure is based on the thermodynamic point of view.

Figure 4: Membrane SEM images of a solution of 15% by weight of EVAL immersed in water without evaporation stage. (A) high- level; (b) cross-section.

a

b
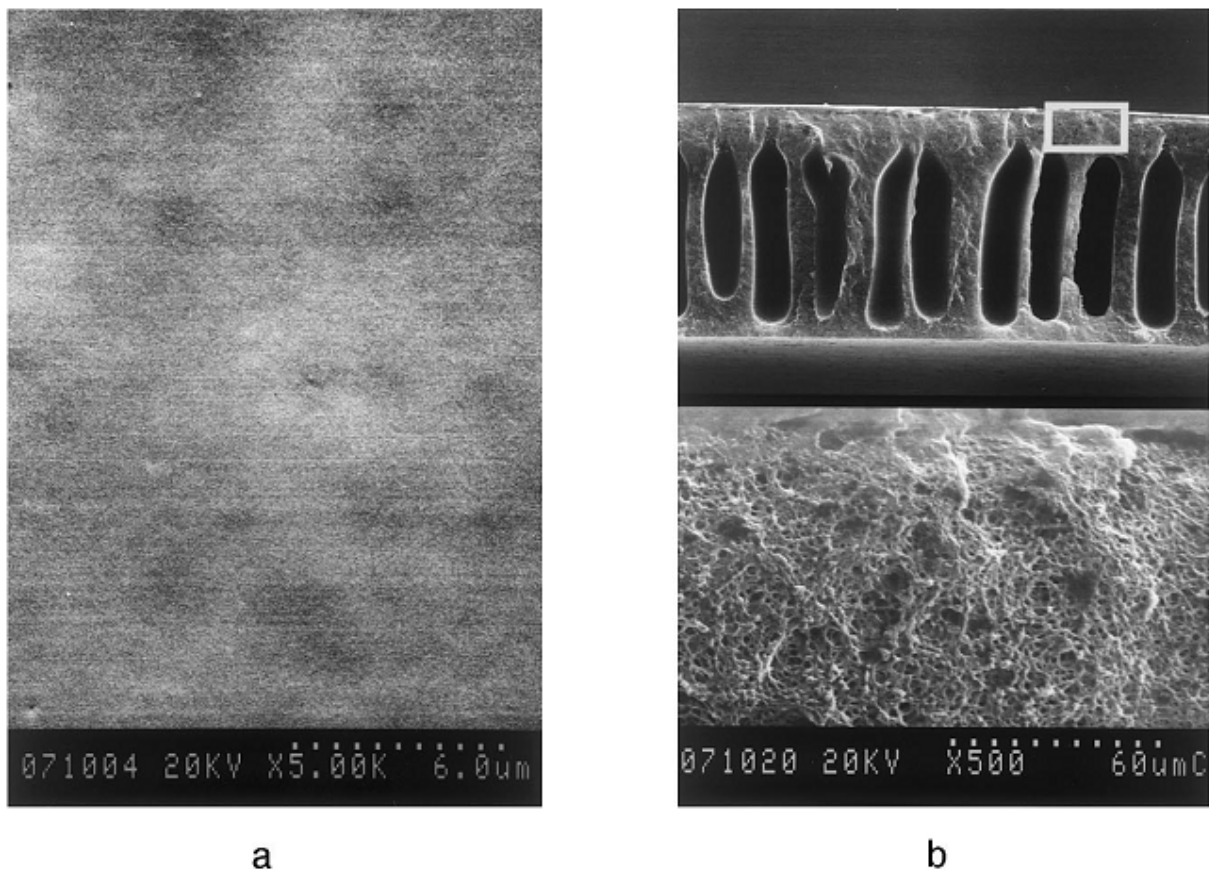
When the evaporation time of 5 minutes was used, the membrane structure for the direct immersion of the casting solution to a water bath without evaporation stage is similar to the membrane (it is not shown here). A dense layer of skin is on the surface of the membrane and the large pores extends to the substrate. This shows that the mechanism of membrane formation is similar in these two systems. Thus, the increase effect of polymer concentration with DMSO evaporation of the casting solution for 5 minutes is not significant in the membrane structure.

When the evaporation time was 15 minutes, the system is still involved liquid-liquid separation that results from the asymmetric morphology with outstanding large pores (It is not shown here). The polymer concentration is almost 20w.t% for 15 minutes of evaporation (Figure 2). This means that the casting solution is still higher than the equilibrium crystallization (Figure 1). Therefore, it is logical that the mechanism of membrane formation is identical in the three high membranes.

Figure 5 shows high and cross-sectional index of membrane with the evaporation time of 30 minutes. The high level of this membrane is in the form of micro-porous skin (Figure 5(a)). When the casting solution contacts with the non-solvent, the high level quickly forms a polymeric layer with high concentration according to the liquid-liquid equilibrium with bath deposition [9, 13]. So, when the cellular nuclei is formed near the skin, it can grow through the skin [22], and the micro-porous skin will be formed. The cross section of this membrane represents the fully cellular structure (Fig. 5 (b)).

Although the immediate separation can be seen in the light transmittance tests (Figure 3), other column fingers are not available.

The mechanism for the formation of finger-like large pores is beyond the scope of the current work.

However, a membrane formation system with an immediate mechanism of liquid-liquid separation is generally in favor of large pore morphology [22].

For this reason, the removal of large pore in the membrane system with immediate liquid-liquid separation may be result from the more viscosity of more concentrated polymer solution in the deposition point that inhibits the growth of large pores [23]. Thus, the increase of polymer concentration with the long evaporation time represents an undesirable situation for the formation of the large pore of the membrane but it is desirable for the formation of sponge membrane.

Figure 5. SEM images of a solution of 15% w.t of EVAL immersed in the water after 30 minutes evaporation (a) high level; (b) cross-section; (c) image magnification of (b)

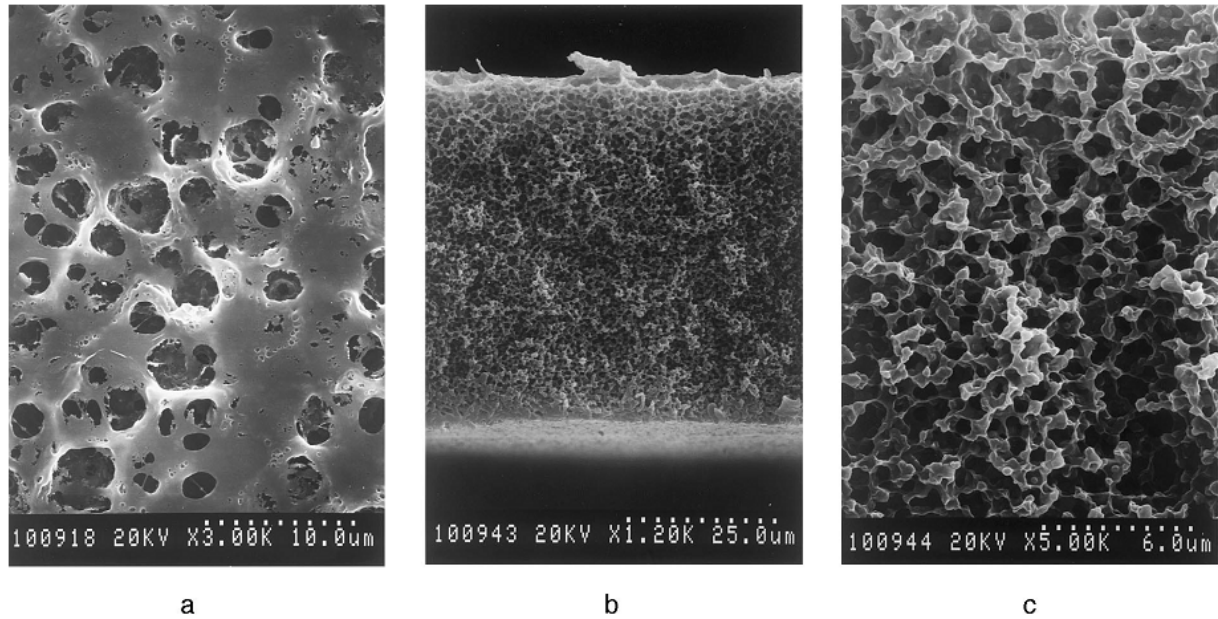a   b   c

Figure 5 (c) shows the details of cellular structure in the higher magnification. The uniformity of the sponge structure shows that it is dominated by the liquid- liquid separation process. Moreover, the cell walls composed of polymer-rich phase are deformed and irregular. Almost all the walls of pores are open and interconnected and lead to a binary continuous structure. Such a morphology may be partly caused by liquid-liquid separation and partly caused by crystallization.

Because the polymer-rich wall is always in the super-saturation state after liquid-liquid separation due to the crystallization (see the phase diagram in Figure 1), the polymer can be crystallized from the amorphous gel in the solid matrix [24]. This indicates that the crystallization occurs in the late stages of deposition and the cellular structure has been largely proved. Thus, this membrane is a cellular structure similar to that of amorphous membrane. The crystallization removes its effect only in the cellular wall. When 45 minutes of evaporation time is used, the membrane structure was undergoing dramatic changes. Unlike the figure 4 (a), this surface is porous and the particles are formed at a high level, as it has been shown in the figure 6 (a). This means that EVAL deposition is not dictated only by the liquid-liquid separation and formation of the particles grain. Because the crystallization is converted to a competitive or even dominance separation phase mechanism for the membrane. As shown in the figures (b) and (c), the cross-section of this membrane is of spherical particles that are intertwined to form a binary continuous network. Cell pores caused by liquid-liquid separation process are not clear.

Figure 6. SEM images of a solution of 15% w.t of EVAL immersed in the water after 45 minutes evaporation (a) high level; (b) cross-section; (c) image magnification of (b).

a   b   c
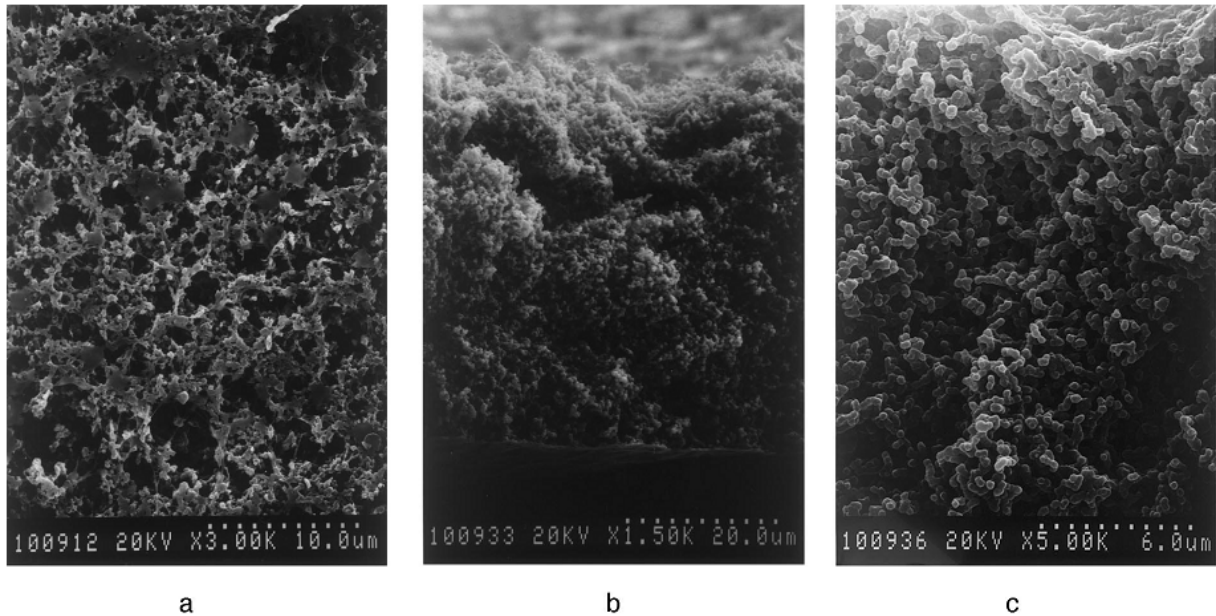
After 60 minutes of long evaporation period, the high-level structure is practically identical with the bulk area of the membrane, as shown in the figure 7. Unlike the membrane with flat and dense structure shown in the figure 6 (a), this level does not show any dense area in total (Figure 7 (a)). Because the cross-sectional structure of membrane is similar to the high-level structure, this membrane is determined by symmetrical and homogenous morphology. At this time, the solid-liquid separation undoubtedly occurs in the membrane with a core and growth mechanism. Then, these cores will be grow until their superficies attack each other to form a particle membrane. Therefore, no cellular morphology has been found due to the liquid-liquid separation.

Figure 7. SEM images of a solution of 15% w.t of EVAL immersed in the water after 60 minutes evaporation (a) high level; (b) cross-section; (c) image magnification of (b).
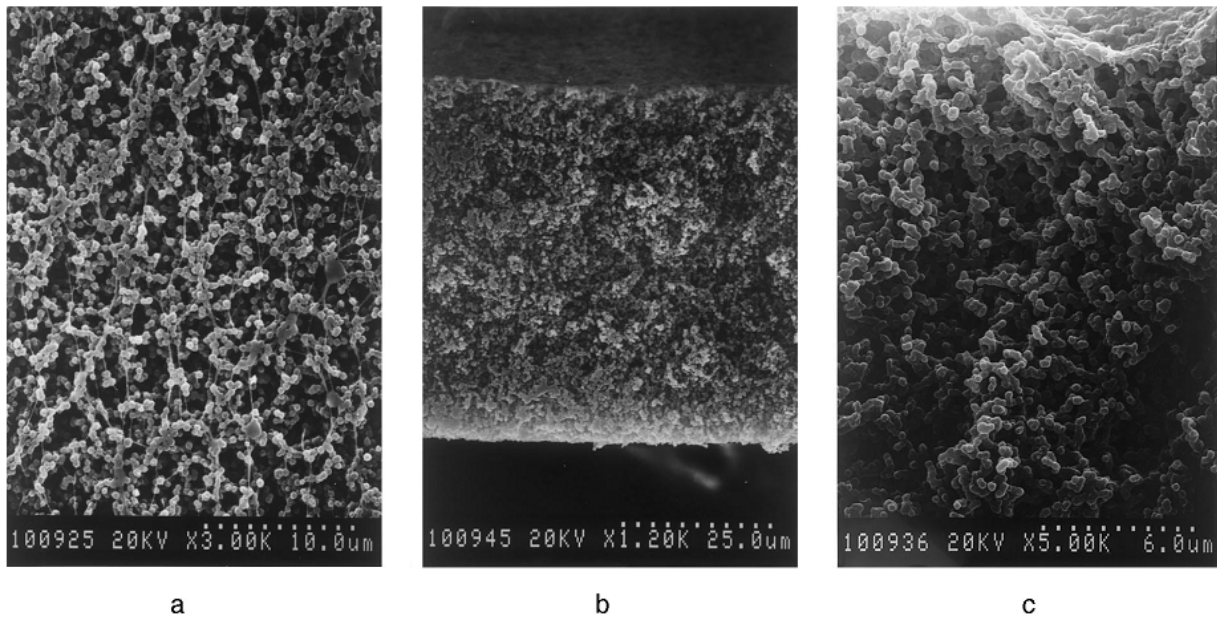

4. Discussion

Membranes of this work show that a wide range of morphologies can be joined with different evaporation periods during the membrane formation. This difference clearly indicates that when the formations of these membranes are identical in the fuzzy diagram, they should have different release kinetics. In particular, liquid-liquid separation and crystallization occur at two different times. So, crystallization may complicate the evaporation effect in the crystalline polymer membrane.

As usual, the composition path for the prepared membrane by the direct deposition process follows the 'a' line in the figure 8. Starting at point "0", a mixture of polymer and solvent, it interrupts the equilibrium crystallization and knots lines with respect to the solvent-non solvent exchange. In these circumstances, the crystallization must happen first, but if the release process is very fast then the time of membrane solution in the liquid-solid separations area is too short in order to allow the crystallization process. As a result, liquid-liquid separation process overcomes the membrane formation mechanism and form an asymmetric membrane with cellular pores.

Figure 8: the comparative paths for solution deposition of 15 % w.t of the EVAL in the water bath (━:
crystallization equilibrium line; ---: two-knot border). (A) Without evaporation; (b) with evaporation. The numbers
show the evaporation time.
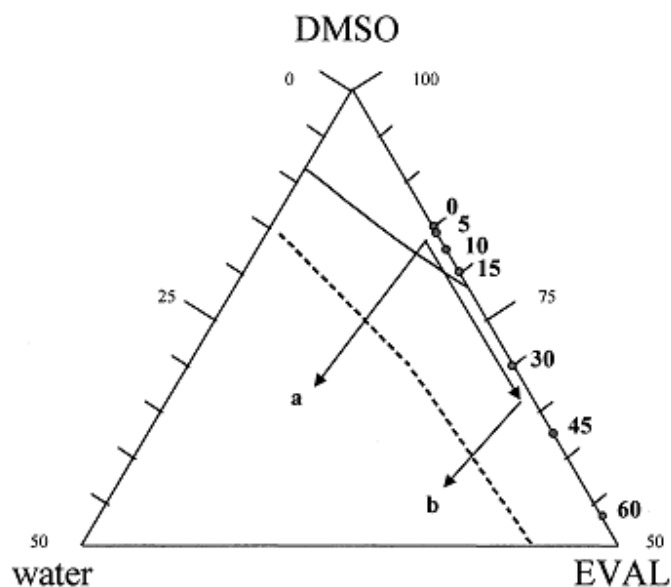
As described above, when there is enough time for the liquid-solid separation, it is expected to occur crystallization. According to this concept, when DMSO leaves the casting solution with the evaporation instead of solvent- non solvent exchange with the diffusion, the composition path follows the "b1" line on figure 8 and it does not pass through the two-knot path. Thus, crystallization has more time to develop. The data point with different times in the figure 8 which is related to the evaporated solution composition in the figure 2 showed that this is a composition above the equilibrium crystallization line in a shorter time of evaporation. About 15 minutes of DMSO evaporation is required for composition path to reach in a liquid-solid separation area. So, when the evaporation time is less than 15 minutes, evaporation solution is still a good solution in which the polymers chains are solved well. Of course, the effect of 15 minutes evaporation is not significant in the membrane structure. In contrast, when the evaporation time increases, the evaporation solution such as 45 and 60 minutes of the evaporation time is related to the crystallization in the metastable state in which the coil is developed into a dense structure. Such a solution containing a large population of new crystal. As a result, the evaporation process increases the system capability for crystallization and special membranes can be produced in this way; see figures 6 and 7. However, it seems that a combination can form nuclei below the equilibrium crystallization.

Such a case was observed when using a 30 minutes of evaporation time. Although, the evaporated solution composition (30 w.t % EVAL in the DMSO) is located in the liquid-solid separation area. The liquid-liquid separation and crystallization will begin almost at a close time. See figure 5. This can be attributed to the fact that nucleation and crystal growth rates increase by raising the polymeric super-saturation degree. In order to describe the exact time of evaporation governing the particle membrane development, the temperature of the crystallization for the 30% w.t solution

of EVAL is about $45^0 C$. See figure 2 in our previous report [8]. Therefore, the temperature of this case is 20 degrees. This result shows that high levels of super-saturation is necessary for the crystallization process in order to dominate the structure of the resulting membrane. Compared to the membranes prepared from the evaporation time of 0-60 minutes, it can be concluded that the membrane structure depends on the occurrence of phase inversion. In addition, the sequence of crystallization and liquid-liquid separation depend on the degree of super-saturation solution. So, it was shown that evaporation stage increases the EVAL ability to crystallize with the polymer concentration increase in order to increase the driving force for crystal nucleation.

Although, the particles core is initiated in the evaporation stage, core growth may be covered by the restrictions on the polymer diffusion in the confined conditions. So, no difference in the light transmittance of a polymer solution can be displayed before and after the evaporation because the core diameter is small compared to the small wavelength of light. After evaporation, the composition path follows the "b2" line in the Fig. 8 by immersing the evaporated solution in the water. In that time, two-knot fusion border is entered. This shows that the liquid-liquid separation process causing the growth of a particle in the next immersion in a water bath.

This growth is stopped during its progress towards the other particles. That is, particle morphology is attributed to the phase passing waterfall. First, the solid-liquid separation form the particles cores. Second, because of the liquid-liquid separation, the particle growth is performed in the core surroundings. So, regardless of the time of evaporation, the overall rate of evaporation is of the experiments of immediate light transmission (Figure 3). However, at this time, liquid-liquid separation plays only a minor role in determining the membrane structure. Because the core formation in the evaporation process determines the structure properties of the resulting membrane.

Finally, a path describes the location compound and the compound dependent on the polymer solution time. However, the gravimetric method is used to measure the change in the composition of the casting solution during the evaporation process and allows to determine only the average composition. So, when concentration gradients may be ignored during the evaporation process, the data in Figure 2 allows us to draw a path of average composition in the triangular phase diagram as shown in Figure 8.

In this work, the crystallization constitutes more cores much lower than the equilibrium crystallization line and particles grow until their superficies attack to each other. Since, the particles size needs to determine the induction time before any development, it seems that the particles in figure 7 have a uniform size that is an evidence of simultaneous nucleation. As a result, when the driving force for crystallization increases with increasing concentration of EVAL, the starting of particle core along the full casting solution occurs simultaneously. Therefore, it is logical that the uniform particle membrane prepared by a Homogeneous mixture in which the difference of small concentration along the membrane could then be ignored.

5. Conclusion

Analysis of the solvent evaporation and phase diagram presents an explanation for the effect of evaporation on the membrane morphology. It seems that when the membrane is immersed in the

bath deposition, its structure is determined by the evaporated solution state. Thus, the given evaporation time for system before the casting solution immersion in the bath deposition is important. The large pores are found in a membrane when EVAL solution is immediately immersed in the water bath or it is immersed with the evaporation time of less than 15 minutes.

When the evaporation time is 30 minutes then the large pores are disappeared. When the evaporation time is 45 or 60 minutes, a skinless and symmetrical membrane is observed by the constituent particles connected to each other. Two effects can describe the solid-liquid separation that occurs at a longer time of the evaporation process. First, the polymer concentration has increased due to the solvent evaporation. The second reason is that the time available for crystallization and to enable the solid-liquid separation is developed. Therefore, the solid-liquid separation can be started with a small core in the evaporation stage. After that, the membrane formation is completed by the liquid-liquid separation in the immersion stage that the particle core has begun to characterize the resulting membrane.

References

[1] M. Mulder, Basic Principles of Membrane Technology, Kluwer Academic Publishers, Dordrecht, 1991.
[2] R.E. Kesting, Synthetic Polymeric Membranes, Wiley, New York, 1985.
[3] J.H. Aubert, Isotactic polystyrene phase diagrams and physical gelation, Macromolecules 21 (1988) 3468–3473.
[4] D.R. Lloyd, K.E. Kinzer, H.S. Tseng, Microporous membrane formation via thermally induced phase separation I.Solid–liquid phase separation, J. Membr. Sci. 52 (1990) 239–261.
[5] A.M.W. Bulte, B. Folkers, M.H.V. Mulder, C.A. Smolders, Membranes of semicrystalline aliphatic polyamide nylon 4,6: formation by diffusion-induced phase separation, J. Appl. Polym. Sci. 50 (1993) 13–26.
[6] L.P. Cheng, A.W. Dwan, C.C. Gryte, Membrane formation by isothermal precipitation in polyamide–formic acid–water system I. Description of membrane morphology, J. Polym.
Sci. Polym. Phys. 33 (1995) 211–222.
[7] P. van de Witte, H. Esselbrugge, P.J. Dijkstra, J.W.A. van de Berg, J. Feijen, A morphological study of membranes obtained from the systems polylactide-dioxane-methanol, polylactide-dioxane-water, and polylactide-N-methyl pyrrolidone-water, J. Polym. Sci. Polym. Phys. 34 (1996) 2569–2578.
[8] T.H. Young, J.Y. Lai, W.M. Yu, L.P. Cheng, Equilibrium phase behavior of the membrane forming water-DMSO-eval copolymer system, J. Membr. Sci. 128 (1997) 55–65.
[9] L.P. Cheng, T.H. Young, Y.M. You, Formation of crystalline EVAL membranes by controlled mass transfer process in water-DMSO–EVAL copolymer systems, J. Membr. Sci. 145 (1998) 77–90.
[10] T.H. Young, L.W. Chen, L.P. Cheng, Membranes with a microparticulate morphology, Polymer 37 (1996) 1305–1310.
[11] D.T. Lin, L.P. Cheng, Y.J. Kang, L.W. Chen, T.H. Young, Effects of precipitation conditions on the membrane morphology and permeation characteristics, J. Membr. Sci. 140 (1998) 185–194.

[12] L.P. Cheng, H.I. Lin, L.W. Chen, T.H. Young, Solute rejection of EVAL membranes with asymmetric and microparticulate morphologies, Polymer 39 (1998) 2135–2142.

[13] A.J. Reuvers, J.W.A. van der Berg, C.A. Smolders, Formation of membranes by means of immersion precipitation Part I. A model to describe mass transfer during immersion precipitation, J. Membr. Sci. 34 (1987) 45–65.

[14] L.P. Cheng, A.W. Dwan, C.C. Gryte, Membrane formation by isothermal precipitation in polyamide–formic acid–water systems I. Description of membrane morphology, J. Polym. Sci. Polym. Phys. 33 (1995) 211.

[15] L.P. Cheng, A.W. Dwan, C.C. Gryte, Membrane formation by isothermal precipitation in polyamide–formic acid–water systems II. Precipitation dynamics, J. Polym. Sci. Polym. Phys. 33 (1995) 223.

[16] C. Castellari, S. Ottani, Preparation of reverse osmosis membranes. A numerical analysis of asymmetric membrane formation by solvent evaporation from cellulose acetate casting solutions, J. Membr. Sci. 9 (1981) 29–41.

[17] L. Zeman, T. Fraser, Formation of air-cast cellulose acetate membranes Part II. Kinetics of demixing and macrovoid growth, J. Membr. Sci. 87 (1994) 267–279.

[18] S.S. Shojaie, W.B. Krantz, A.R. Greenberg, Dense polymer film and membrane formation via the dry-cast process Part II. Model validation and morphological studies, J. Membr. Sci. 94 (1994) 281–298.

[19] R.Y.M. Huang, X. Feng, Studies on solvent evaporation and polymer precipitation pertinent to the formation of asymmetric polyetherimide membranes, J. Appl. Polym. Sci. 57 (1995) 613–621.

[20] T.H. Young, D.T. Lin, L.Y. Chen, Y.H. Huang, W.Y. Chiu, Membranes with a particulate morphology prepared by a dry–wet process, Polymer 40 (1999) 5257–5264.

[21] W.B. Krantz, R.J. Ray, R.L. Sani, K.J. Gleason, Theoretical study of the transport process occurring during the evaporation step in asymmetric membrane casting, J. Membr. Sci. 29 (1986) 11–36.

[22] C.A. Smolders, A.J. Reuvers, R.M. Boom, I.M. Wienk, Microstructures in phase inversion membranes Part 1. Formation of macrovoids, J. Membr. Sci. 73 (1992) 259–275.

[23] H. Strathmann, K. Kock, P. Pmar, R.W. Baker, The formation mechanism of asymmetric membranes, Desalination 16 (1975) 179–203.

[24] T.H. Young, D.M. Wang, C.C. Hsieh, L.W. Chen, The effect of the second phase inversion on microstructures in phase inversion EVAL membranes, J. Membr. Sci. 146 (1998) 169–178.